

# How to Cache in Mobile Hybrid IoT Networks?

Trung-Anh Do, Sang-Woon Jeon, *Member, IEEE*,  
and Won-Yong Shin, *Senior Member, IEEE*

## Abstract

Content-centric *mobile hybrid* Internet-of-Things (IoT) networks consisting of mobile devices and static femto access points (FAPs) are studied, where each device moves according to the random walk mobility model and requests a content object from the library independently at random according to a Zipf popularity distribution. Instead of allowing access to content objects at macro base stations via costly backhaul providing connection to the core network, we consider a more practical scenario where mobile devices and static FAPs, each having a *finite-size* cache space, are able to cache a subset of content objects so that each request is served by other mobile devices or static FAPs. Under a general multihop-based content delivery protocol, we analyze the order-optimal throughput–delay trade-off by presenting a new cache allocation strategy. In particular, under a given caching strategy, we first characterize a throughput–delay trade-off in terms of scaling laws along with the general content delivery multihop routing protocol. Then, the order-optimal throughput–delay trade-off is characterized by presenting the order-optimal cache allocation strategy, which jointly finds the replication sets at mobile devices and static FAPs via a novel variable decoupling approach. In our mobile IoT network, an interesting observation is that highly popular content objects are mainly served by mobile devices while the rest of content objects are served by static FAPs. We perform numerical evaluation to validate our analytical results. We also show that the order-optimal strategy strictly outperforms a baseline approach, where the replication sets at mobile devices and static FAPs are optimized separately.

## Index Terms

Caching, content-centric network, mobile IoT network, throughput–delay trade-off, variable decoupling.

## 1 INTRODUCTION

Wireless data caching [2] has emerged as a promising technique that effectively deals with the exponential growth of data traffic caused by mobile Internet-of-Things (IoT) devices [3], [4], [5] without introducing costly backhaul (or infrastructure) providing connection to the core network, while maintaining the sustainability of future wireless networks. The core of wireless data caching in content-centric IoT networks is to allow base stations or end terminals to cache a subset of content objects. Hence, user requests can be directly served by base stations or end terminals that have cached the requested objects, without contacting costly backhaul links.

### 1.1 Prior Work

As the number of users continues to grow dramatically, the capacity scaling law behavior has been widely studied in large-scale IoT networks. Gupta and Kumar showed in [6] that for a static IoT network consisting of  $n$  randomly distributed source–destination (S–D) pairs in a unit network area, the per-device throughput of  $\Theta\left(\frac{1}{\sqrt{n \log n}}\right)$  is achievable using the nearest neighbor multihop transmission. There have been further studies on multihop schemes in the literature [7], [8], [9], [10], where the per-device throughput scales far slower than  $\Theta(1)$ . Besides the multihop schemes, there have been various research directions to improve the per-device throughput up to a constant scaling by using hierarchical cooperation [11], device mobility [12], [13], directional antennas [14], [15], [16], and infrastructure support [17], [18].

Contrary to the studies on the conventional IoT network model in which S–D pairs are given and fixed, investigating *content-centric IoT networks* would be quite challenging. As content objects are cached by numerous mobile IoT devices over a network, finding the closest content holder of each request and scheduling between requests are of crucial importance for improving the overall network performance. The scaling behavior of content-centric IoT networks has received a lot of attention in the literature [19], [20], [21], [22], [24], [26]. In *static* ad hoc networks, throughput scaling laws were analyzed using multihop communication [19], [21], which yields a significant performance gain over the single-hop caching scenario in [2], [20]. More specifically, a centralized and deterministic cache allocation strategy was presented in [19], where replicas

*The material in this paper was presented in part at the IEEE International Symposium on Information Theory, Barcelona, Spain, July 2016 [1]. (Corresponding author: Won-Yong Shin.)*

*T.-A. Do was with Dankook University, Yongin 16890, Republic of Korea. He is now with the Division of Science and Technology Management and International Cooperation, Posts and Telecommunications Institute of Technology, Hanoi 100000, Vietnam (e-mail: anhdt@ptit.edu.vn).*

*S.-W. Jeon is with the Department of Military Information Engineering, Hanyang University, Ansan 15588, Republic of Korea (e-mail: sangwoon-jeon@hanyang.ac.kr).*

*W.-Y. Shin is with the Department of Computer Science and Engineering, Dankook University, Yongin 16890, Republic of Korea (e-mail: wyshin@dankook.ac.kr).*

of each content object are statically determined based on the popularity of each content object in a centralized manner. A decentralized and random cache allocation strategy along with a local multihop protocol was also introduced in [21], where content objects are assigned independently at random to the caches of all users. On the other hand, in *mobile* IoT networks, performance on the throughput and delay was examined under a reshuffling mobility model, where the position of each mobile device is independently determined according to random walks with an adjustable flight size and updated at the beginning of each time slot [22]. Alfano et al. showed in [22] that increasing the mobility degrees of mobile devices leads to worse performance when deterministic cache allocation is used similarly as in [19]. In [23], the above performance analysis was then extended to the case where the size of each content object is considerably large and thus only a subpacket of a file can be delivered during one time slot. Performance on the throughput and delay was also investigated in [24] under a correlated mobility model, where mobile devices are partitioned into multiple clusters and the devices belonging to the same cluster move in a correlated fashion. Liu et al. showed in [24] how correlated mobility affects the network performance. In addition, caching in IoT networks was extended to *static* infrastructure-supported IoT networks using multihop communication [25], [26]—each macro base station was assumed to be connected to the core network via infinite-speed backhaul, which has an access to all content objects stored in the whole file library.

Meanwhile, a different caching framework, termed coded caching [27], [28], [29], has received a great deal of attention in cache-enabled wireless networks, where a single transmitter simultaneously deals with several different demands using common coded multicast transmission. Based on this approach, a global caching gain can be achieved by finding the optimal content placement such that multicasting opportunities are exploited simultaneously for all possible requests in the delivery phase.

## 1.2 Main Contributions

In this paper, we study a large-scale content-centric *mobile hybrid multihop IoT* network, where each mobile device moves according to the random walk mobility model (RWMM) and requests a content object from the library independently at random according to a Zipf popularity distribution while multiple femto access points (FAPs) (or helper devices) are regularly placed over the network area. Instead of assuming an access to the core network through infinite-speed backhaul links as in [26], we assume that *each of mobile devices and FAPs is equipped with a finite-size cache* and is able to cache content objects in the library. Our caching framework is basically composed of the caching phase and the delivery phase. For a given caching strategy, we first present a content delivery routing protocol with and without FAP support via multihop in order to deliver content objects to requesting mobile devices, which leads to a fundamental throughput–delay trade-off. Then, we optimize a cache allocation strategy that provides the order-optimal throughput–delay trade-off. Specifically, we propose a novel *variable decoupling* approach that optimally finds the replication sets for caching at mobile devices and static FAPs, denoted by  $A_m$  and  $B_m$  for content object  $m \in \{1, \dots, M\}$ , respectively, where  $M$  indicates the number of content objects in the library. The proposed approach solves two different convex optimization problems with relaxation based on the relative size of  $A_m$  and  $B_m$ , leading to much simpler analysis without loss of order optimality compared to tackling the original problem that may not provide a tractable closed-form solution. In our mobile IoT network, main results reveal that when each FAP has a relatively large-size cache, highly popular content objects are mainly served by mobile devices whereas the rest of content objects are served by static FAPs. Based on the order-optimal cache allocation strategy, we finally characterize the order-optimal throughput–delay trade-off with respect to system parameters.

The main contributions of this paper are summarized as follows:

- For comprehensive understanding of content-centric IoT networks, we present a general framework in which both static FAPs and mobile devices are able to cache a subset of content objects with different capabilities, also capturing the effects of user mobility and multihop content delivery.
- Under such a general setting, the order-optimal throughput–delay trade-off is analyzed, which is the first result that characterizes a fundamental trade-off between throughput and delay of content-centric mobile IoT networks.
- The main technical challenge resides in establishing the order-optimal content replication strategy (i.e., the order-optimal cache allocation strategy), which jointly optimizes the number of replicas cached at mobile devices and static FAPs, denoted by  $A_m$  and  $B_m$  for  $m \in \{1, \dots, M\}$ , respectively. An interesting observation is that when the total cache space at all FAPs is greater than that at all mobile devices, highly popular contents are stored mainly in mobile device caches while any request for less popular contents is fulfilled by static FAPs.
- Our analytical solution for the order-optimal caching placement is compared with a numerically optimized solution, demonstrating that our scaling law analysis is well matched with the numerical results.
- For comparison, a baseline strategy that optimizes the replication sets at mobile devices and static FAPs in a separate manner is further presented and shows that it is strictly suboptimal.

## 1.3 Organization

The rest of this paper is organized as follows. In Section II, the network model and performance metrics under consideration are described. In Section III, the content delivery routing protocol is presented. In Section IV, a fundamental throughput–delay trade-off is introduced in terms of scaling laws. In Section V, the order-optimal throughput–delay trade-off is derived by introducing the order-optimal cache allocation strategy using variable decoupling. In Section VI, numerical results are shown for validation. A baseline strategy is also shown in Section VII for comparison. Finally, Section VIII summarizes the paper with some concluding remarks.

## 1.4 Notations

Throughout this paper,  $\mathbb{E}[\cdot]$  and  $\Pr(\cdot)$  are the expectation and the probability, respectively. Unless otherwise stated, all logarithms are assumed to be to the base 2. We also use the following asymptotic notation: i)  $f(x) = O(g(x))$  means that there exist constants  $C$  and  $c$  such that  $f(x) \leq Cg(x)$  for all  $x > c$ ; ii)  $f(x) = o(g(x))$  means that  $\lim_{x \rightarrow \infty} \frac{f(x)}{g(x)} = 0$ ; iii)  $f(x) = \Omega(g(x))$  if  $g(x) = O(f(x))$ ; iv)  $f(x) = \omega(g(x))$  if  $g(x) = o(f(x))$ ; and v)  $f(x) = \Theta(g(x))$  if  $f(x) = O(g(x))$  and  $f(x) = \Omega(g(x))$  [30]. That is,  $f(x) = O(g(x))$  means that  $g(x)$  increases faster than or equal to  $f(x)$  in an order sense. Similarly,  $f(x) = o(g(x))$  means that  $g(x)$  increases strictly faster than  $f(x)$  in an order sense. Lastly,  $f(x) = \Omega(g(x))$  means that  $f(x)$  and  $g(x)$  increase with the same order.

## 2 NETWORK MODEL AND PERFORMANCE METRICS

In this section, we first describe the network model and then define performance metrics used in the paper.

### 2.1 Network Model

We consider a content-centric mobile hybrid IoT network consisting of  $n$  mobile devices and  $f(n) = \Theta(n^\delta)$  static FAPs (or static helper devices), where  $0 \leq \delta < 1$ , which is a general network model including the prior models [2], [13], [19], [20], [21], [22], [26]. We assume that  $n$  mobile devices are distributed uniformly at random over a unit square and  $f(n)$  FAPs are regularly placed over the same area. That is, the network is divided into  $f(n)$  square femto cells of equal size given by  $b(n) = \Theta\left(\frac{1}{f(n)}\right)$  so that each cell has one FAP at its center. The mobility trace of devices is modelled according to the RWMM as in [13], [31]. In particular, the unit area is divided into  $n$  square subcells of area  $\frac{1}{n}$ . Each mobile device independently performs a simple random walk with a distance  $\frac{1}{\sqrt{n}}$  on the  $\sqrt{n} \times \sqrt{n}$  disjoint subcells so that the mobile device is equally likely to be in any of the four adjacent subcells after each time slot.

In our content-centric mobile IoT network, each mobile device and static FAP are assumed to be equipped with local caches, which are installed to store a subset of content objects in the central server with a database of  $M = \Theta(n^\gamma)$  content objects, where  $0 < \gamma < 1$ . Every content object is assumed to have the same size. In this paper, we consider a more practical cache-enabled network model by assuming that each device and FAP are able to cache at most  $K_n = \Theta(1)$  and  $K_{FAP} = \Theta(n^\beta)$  content objects in their own finite-size caches, respectively, where  $0 < \beta < \gamma$ . We focus on the case that the total cache size in static FAPs scales no slower than the total cache size of mobile devices in the network, i.e.,  $\delta + \beta \geq 1$ , in order to analyze the impact and benefits of FAPs equipped with a relatively large-size cache.<sup>1</sup>

We assume that every mobile device requests its content object independently according to a Zipf popularity distribution, which typically characterizes a popularity of various kinds of real data such as web, file sharing, user-generated content, and video on demand [32].<sup>2</sup> That is, the request probability of content object  $m \in \mathcal{M} \triangleq \{1, \dots, M\}$  is given by<sup>3</sup>

$$p_m = \frac{m^{-\alpha}}{H_\alpha(M)}, \quad (1)$$

where  $\alpha > 0$  is the Zipf exponent and  $H_\alpha(M) = \sum_{i=1}^M i^{-\alpha}$  is a normalization constant formed in the Riemann zeta function and is given by

$$H_\alpha(M) = \begin{cases} \Theta(1) & \text{for } \alpha > 1 \\ \Theta(\log M) & \text{for } \alpha = 1 \\ \Theta(M^{1-\alpha}) & \text{for } \alpha < 1. \end{cases} \quad (2)$$

In content-centric networks, a caching problem is generally partitioned into the caching phase and the delivery phase. That is, the problem consists of storing content objects in the caches and establishing efficient delivery routing paths for the requested content objects.

We first consider the caching phase, which takes place during off-peak periods to proactively select the content objects from the central server to be stored in the caches of  $n$  devices and  $f(n)$  FAPs. Let  $A_m$  and  $B_m$  denote the number of replicas of content object  $m \in \mathcal{M}$  stored at mobile devices and static FAPs, respectively, which will be optimized later. In order for a cache allocation to be feasible,  $\{A_m\}_{m=1}^M$  and  $\{B_m\}_{m=1}^M$  should satisfy the following total caching constraints:

$$\begin{cases} \sum_{m=1}^M A_m \leq nK_n, \\ \sum_{m=1}^M B_m \leq f(n)K_{FAP}. \end{cases} \quad (3)$$

Furthermore, we impose the following individual caching constraints:

$$\begin{cases} A_m \leq n, \\ B_m \leq f(n), \\ A_m + B_m \geq 1 \end{cases} \quad (4)$$

1. Otherwise, the use of FAPs would not be beneficial in improving performance on the throughput and delay in our network model.
2. Note that a Zipf popularity has also widely been adopted in mobile IoT networks [33], [34].
3. Without loss of generality, we assume a descending order between the request probabilities of the  $M$  content objects in the library.

for all  $m \in \mathcal{M}$ . Note that the last constraint in (4) is needed to avoid an outage event such that a requested content object is not stored in the entire network. Similarly as in [19], [22], we employ the *random caching* strategy such that the sets of replicas satisfying (3) and (4) are stored uniformly at random over the caches in  $n$  devices and  $f(n)$  FAPs.

Now, let us consider the delivery phase of the requested content objects, which allows the requested content objects to be delivered to the corresponding mobile devices over wireless channels. During the delivery phase, each mobile device downloads its requested content object (possibly via multihop) from one of the mobile devices or static FAPs storing the requested content object in their caches. We adopt the *protocol model* [6] for successful content delivery. In particular, let  $d(u, v)$  denote the Euclidean distance between devices  $u$  and  $v$ . Then, content delivery from device  $u$  to device  $v$  is assumed to be successful if and only if  $d(u, v) \leq r$  and there is no other active transmitter in a circle of radius  $(1 + \Delta)r$  from device  $v$ , where  $r$  and  $\Delta > 0$  are given protocol parameters.

For analytical tractability, we also adopt the *fluid model* in [13]. In this model, the size of each content object is assumed to be arbitrarily small. Accordingly, the time required for delivery of one content between a device and its neighbor device or an assigned FAP is much smaller than the duration of each time slot. In this case, the data sent from a device in one time slot may correspond to multiple content objects, and thus all content objects waiting for transmission at a device will be transmitted by the device within one time slot. However, a content object received by a device in a given time slot cannot be transmitted by the device until the next time slot.

## 2.2 Performance Metrics

Since every content object is assumed to have the same size, we consider the per-device throughput  $\lambda(n)$ , i.e., the rate at which the request of any mobile device in the network can be served according to a given feasible content delivery routing. We make slight modifications to the definitions of throughput and delay in [13] to fit into our content-centric mobile IoT network, which are provided as follows.

**Definition 1** (Throughput). Let  $B(i, t)$  denote the total number of bits of the requested content objects received by device  $i$  during  $t$  time slots. Note that this could be a random quantity for a given network realization. Then, the per-device throughput  $\lambda(n)$  is said to be achievable if there exists a sequence of events  $A(n)$  such that

$$A(n) = \left\{ \min_{1 \leq i \leq n} \liminf_{t \rightarrow \infty} \frac{1}{t} B(i, t) \geq \lambda(n) \right\}$$

and  $\Pr(A(n))$  approaches one as  $n$  tends to infinity.

**Definition 2** (Delay). Let  $D(i, k)$  denote the delay of the  $k$ th requested content object of device  $i$ , which is measured from the moment that the requesting message leaves device  $i$  until the corresponding content object arrives at the device from the closest holder. For a particular realization of the network, the delay for device  $i$  is  $\limsup_{q \rightarrow \infty} \frac{1}{q} \sum_{k=1}^q D(i, k)$  for a sufficiently large number of requested content objects of the device. Then, the delay is defined as the expectation of the average delay of all devices over all network realizations, i.e.,

$$D(n) \triangleq \mathbb{E} \left[ \frac{1}{n} \sum_{i=1}^n \limsup_{q \rightarrow \infty} \frac{1}{q} \sum_{k=1}^q D(i, k) \right].$$

## 3 CONTENT DELIVERY ROUTING PROTOCOL IN MOBILE HYBRID IOT NETWORKS

In this section, we describe our routing protocol to deliver content objects to requesting mobile devices. Due to the device mobility, our routing protocol is basically built upon the nearest neighbor multihop routing scheme in [13] and reconstructed for our cache-enabled setting accordingly. For multihop transmission, the network of unit area is divided into  $a(n)^{-1}$  square routing cells of equal size, where  $a(n) = \Omega\left(\frac{\log n}{n}\right)$  and  $a(n) = O(1)$ , so that each routing cell has at least one mobile device with high probability (whp) (see [6] for the details). We implement a multihop routing strategy for content delivery based on *routing cells* and *femto cells* whose size is  $a(n)$  and  $b(n)$ , respectively. Each routing cell is activated regularly once every  $1 + c$  time slots to avoid any collision, where  $c > 0$  denotes a small integer independent of  $n$ . Similarly, each femto cell is activated regularly once every  $1 + c$  time slots.

The requesting mobile device first finds its closest holder (in the Euclidean distance) of the desired content object among  $A_m$  devices and  $B_m$  FAPs. Then, a requesting message is delivered to the closest holder along the adjacent routing cells via multihop in forward direction, which corresponds to the first phase of the content delivery. Similarly, the desired content object chases the requesting device moving according to the RWMM via multihop in backward direction, which corresponds to the second phase. Each time slot is divided into two sub-slots. The first and second phases of the content delivery procedure are activated during the first and the second sub-slots, respectively. For the case where the requesting mobile device is inside the transmission range of any holder of the desired content object, the request will be served using single-hop transmission within one time slot. The detailed content delivery procedure is described as follows:

### Step 1) Requesting phase

- a) If the closest holder is a mobile device, then the requesting message chases the target device according to the following procedure. As depicted in Fig. 1(a), from routing cell  $C^0$ , the requesting message is transmitted via multihop along

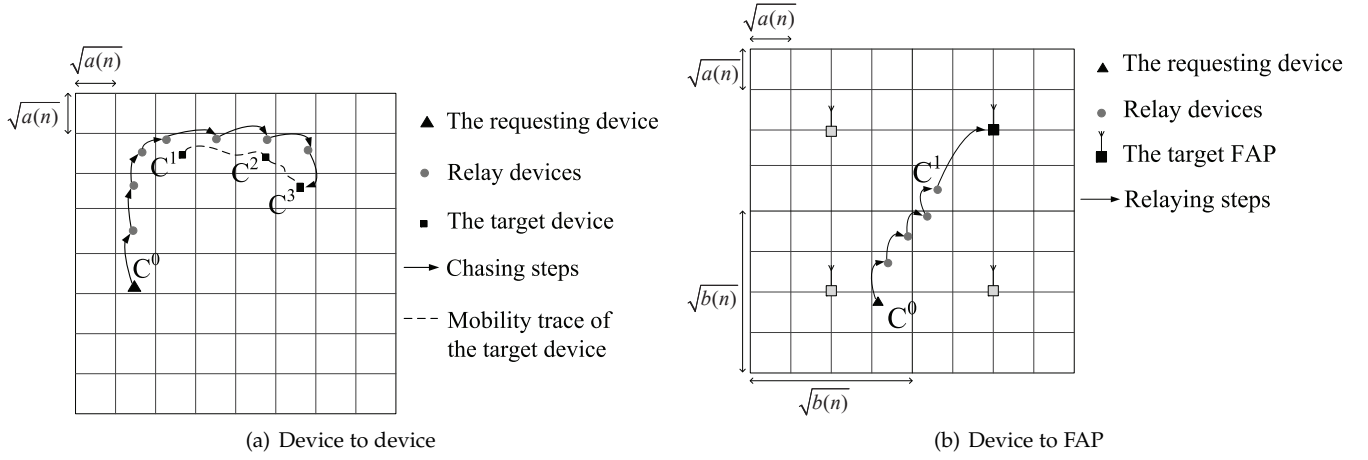


Fig. 1: The first phase of the content delivery routing.

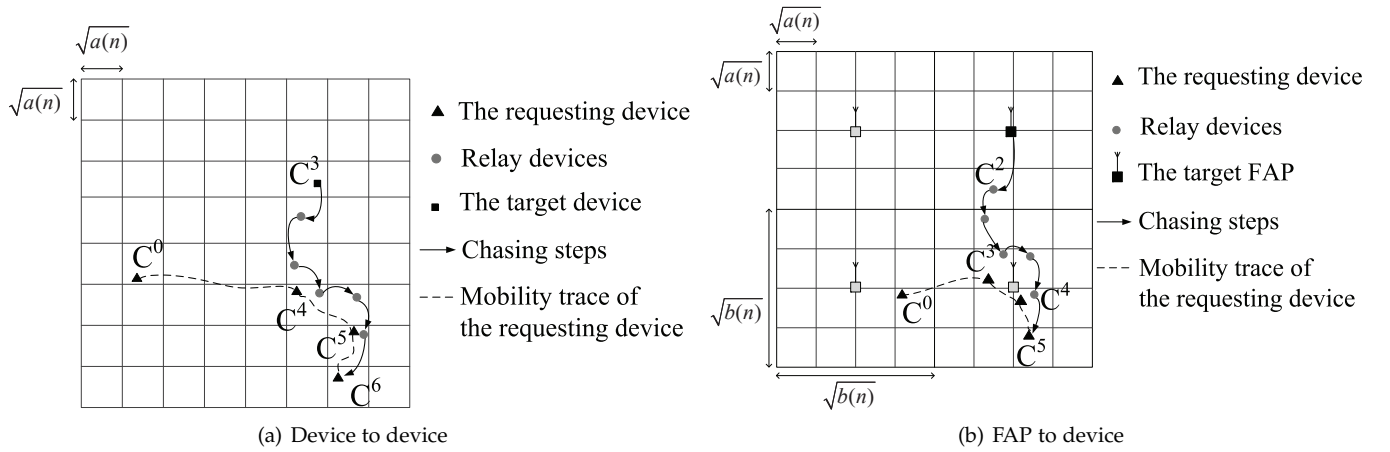


Fig. 2: The second phase of the content delivery routing.

the adjacent routing cells toward routing cell  $C^1$  containing the target device, where the per-hop distance is given by  $\Theta(\sqrt{a(n)})$ . By the time the requesting message reaches routing cell  $C^1$ , the target device has moved to another position  $C^2$  with the mobility trace based on the RWMM. Thus, the message hops from routing cell  $C^1$  to routing cell  $C^2$ . This continues until the message reaches the routing cell  $C^3$  containing its target device.

- b) As depicted in Fig. 1(b), if the closest holder is an FAP, then the requesting message is delivered via multihop along the adjacent routing cells intersecting the straight line toward the coverage of the target FAP, where the per-hop distance is given by  $\Theta(\sqrt{a(n)})$ . When the requesting message arrives at a mobile device in routing cell  $C^1$  that is inside the FAP cell coverage of the target FAP, the last relay device will send the message to the FAP immediately using single-hop within one time slot, where the last hop distance to the target FAP is given by  $\Theta(\sqrt{b(n)})$ . This long-distance hop for the last hop to the FAP leads to the best performance (which will be specified later).

### Step 2) Delivery phase

- a) By the time the target device receives the requesting message, the requesting device has moved to another position  $C^4$  with the mobility trace based on the RWMM. As illustrated in Fig. 2(a), the desired content object delivered by the target device chases the requesting device by executing essentially the same procedure as the first delivery phase.
- b) By the time the FAP receives the requesting message, the requesting device has moved to another position  $C^3$ . As illustrated in Fig. 2(b), the desired content object delivered by the FAP is delivered to a relay device in routing cell  $C^2$  along another straight line toward the requesting device within one time slot. Thereafter, the relay chases the requesting device via multihop until reaching the routing cell containing the requesting device.

The overall procedure of the proposed content delivery routing protocol is summarized in Algorithm 1.

---

**Algorithm 1** The proposed content delivery routing protocol
 

---

- 1: Step 1. First phase (requesting phase)
    - 2: Step 1-1. Device-to-device transmission
    - 3: **if** the closest holder is an FAP **then**
  - 4:     Step 1-2. Device-to-FAP transmission
  - 5: **end if**
  - 6: Step 2: Second phase (delivery phase)
    - 7: **if** the closest holder is an FAP **then**
  - 8:     Step 2-1. FAP-to-device transmission
  - 9: **end if**
  - 10: Step 2-2. Device-to-device transmission
- 

#### 4 THROUGHPUT–DELAY TRADE-OFF

In this section, we characterize a fundamental throughput–delay trade-off in terms of scaling laws for the content-centric mobile hybrid IoT network using the proposed content delivery routing. As stated in Section 3, we consider the nearest neighbor multihop transmission between a requesting device and its closest holder of the desired content object, where their distance is crucially determined by the total number of replicas of content object  $m \in \mathcal{M}$ ,  $A_m + B_m$ . When replicas of each content object are independently and uniformly distributed in the caching phase, the average Euclidean distance from a requesting device to its closest holder was shown to scale as the reciprocal of the square root of the total number of holders of the desired content object in the network (refer to [13], [26] for more details). By applying this argument to our network framework, we establish the following lemma, which is essential to characterize the throughput–delay trade-off.

**Lemma 1.** *For any mobile device requesting content object  $m \in \mathcal{M}$ , the average initial distance between any requesting device and its closest holder of content object  $m$  is  $\Theta\left(\frac{1}{\sqrt{A_m+B_m}}\right)$ , where  $A_m$  and  $B_m$  are the number of replicas of content object  $m$  stored at devices and FAPs, respectively.*

*Proof:* The detailed proof of this argument is omitted here since it basically follows the same line as the proof of [26, Lemma 3] with a slight modification.  $\square$

We are now ready to show our first main result.

**Theorem 1.** *Suppose that the content delivery routing in Section 3 is used for the content-centric mobile hybrid IoT network. Then, the throughput–delay trade-off is given by*

$$\lambda(n) = \Theta\left(\frac{D(n)}{n\left(\sum_{m=1}^M \frac{p_m}{\sqrt{A_m+B_m}}\right)^2}\right) \quad (5)$$

whp, where

$$\lambda(n) = O\left(\frac{1}{\sum_{m=1}^M p_m \sqrt{\frac{n \log n}{A_m+B_m}}}\right)$$

and  $p_m$  is the request probability of content object  $m \in \mathcal{M}$ .

*Proof:* We compute the initial distance of a randomly selected S–D pair into our cache-enabled network setting. The length of the routing path of a requesting message or a desired content object is shown to be determined by the initial distance between a requesting device and its closest holder of the desired content object, which is given by  $\Theta\left(\frac{1}{\sqrt{A_m+B_m}}\right)$  from Lemma 1. As a result, the total number of hops along the routing paths of both the requesting message and desired content object scales as  $\Theta\left(\frac{1}{\sqrt{a(n)(A_m+B_m)}}\right)$ . Since in our network, the average delay  $D(n)$  is determined by the time taken from the moment that the requesting message leaves until the desired content object arrives at the requesting device, we have

$$D(n) = \Theta\left(\sum_{m=1}^M \frac{p_m}{\sqrt{a(n)(A_m+B_m)}}\right), \quad (6)$$

where  $p_m$  is the probability that each device requests content object  $m \in \mathcal{M}$ .

Similarly as in [13], from the fact that the number of content objects passing through an arbitrary routing cell in each

time slot is given by  $O\left(n \sum_{m=1}^M p_m \sqrt{\frac{a(n)}{A_m + B_m}}\right)$  whp, the average per-device throughput is given by

$$\lambda(n) = \Theta\left(\frac{1}{n \sum_{m=1}^M p_m \sqrt{\frac{a(n)}{A_m + B_m}}}\right) \text{ whp,} \quad (7)$$

which is maximized when  $a(n) = \Theta\left(\frac{\log n}{n}\right)$ . Hence, using (6) and (7) leads to (5), which completes the proof of the theorem.  $\square$

Theorem 1 implies that the throughput–delay trade-off is influenced by the total number of replicas of each content object  $m$ , i.e.,  $A_m + B_m$ . Due to the caching constraints in (3) and (4), it is not straightforward how to optimally allocate the sets of replicas,  $\{A_m\}_{m=1}^M$  and  $\{B_m\}_{m=1}^M$ , to show a net improvement in the overall throughput–delay trade-off. In the next section, we introduce the order-optimal cache allocation strategy to characterize the order-optimal throughput–delay trade-off.

**Remark 1.** *Based on the above result, it is not difficult to show that if content delivery is performed via multihop, then the throughput–delay trade-off for mobile IoT networks is identical to that for static IoT networks in [26]. That is, we may conclude that performance on the throughput–delay trade-off of both cache-enabled networks is the same as far as the content delivery multihop routing protocols are employed.*

According to the same analysis in [26], it is not difficult to show that when  $\alpha \geq 3/2$ , the order-optimal throughput–delay trade-off in Theorem 1 is given by  $\lambda(n) = \Theta(D(n))$  by using device-to-device multihop communication without FAP support. Therefore, for the rest of this paper, we focus on the case where  $\alpha < 3/2$  in solving the optimal content replication problem.

## 5 ORDER-OPTIMAL CACHE ALLOCATION STRATEGY IN MOBILE HYBRID IOT NETWORKS

In this section, we characterize the order-optimal throughput–delay trade-off of the content-centric mobile hybrid IoT network by optimally selecting the replication sets  $\{A_m\}_{m=1}^M$  and  $\{B_m\}_{m=1}^M$  in terms of scaling laws. We first introduce our problem formulation in terms of maximizing the throughput–delay trade-off. Then, we propose a content replication strategy that jointly finds the number of replicas cached at mobile devices and static FAPs, thus leading to the order-optimal throughput–delay trade-off of our network. Finally, We validate our analysis by numerically showing our optimal solution to the cache allocation problem.

### 5.1 Problem Formulation

From Theorem 1, it can be shown that maximizing the throughput–delay trade-off is equivalent to maximizing the throughput  $\lambda(n)$  for given delay  $D(n)$ . Thus, from the caching constraints in (3) and (4), we formulate the following optimization problem:

$$\max_{\{A_m\}_{m=1}^M, \{B_m\}_{m=1}^M} \lambda(n) \quad (8a)$$

$$\text{subject to} \quad \sum_{m=1}^M A_m \leq nK_n, \quad (8b)$$

$$\sum_{m=1}^M B_m \leq f(n)K_{FAP}, \quad (8c)$$

$$A_m \leq n \text{ for } m \in \mathcal{M}, \quad (8d)$$

$$B_m \leq f(n) \text{ for } m \in \mathcal{M}, \quad (8e)$$

$$A_m + B_m \geq 1 \text{ for } m \in \mathcal{M}. \quad (8f)$$

Since maximizing  $\lambda(n)$  for given  $D(n)$  is equivalent to minimizing the term  $n\left(\sum_{m=1}^M \frac{p_m}{\sqrt{A_m + B_m}}\right)$  in (5), the original problem in (8) can be rewritten as

$$\min_{\{A_m\}_{m=1}^M, \{B_m\}_{m=1}^M} \sum_{m=1}^M \frac{p_m}{\sqrt{A_m + B_m}} \quad (9a)$$

$$\text{subject to} \quad (8b)–(8f). \quad (9b)$$

From the fact that the second derivatives of the objective function (9a) with respect to  $A_m$  and  $B_m$  for  $\forall m \in \mathcal{M}$  are non-negative, it is straightforward to preserve the convexity of the objective function. Note that the numbers of replicas of content object  $m$  stored at mobile devices and static FAPs, corresponding to  $A_m$  and  $B_m$ , respectively, are integer variables, which makes the optimization problem non-convex and thus intractable. However, as long as scaling laws are concerned in this work, the discrete variables  $A_m$  and  $B_m$  for  $m \in \mathcal{M}$  can be relaxed to real numbers in  $[1, \infty)$  so that the objective

function in (9a) becomes convex and differentiable. In addition, since all inequality constraints (8b)–(8f) are linear functions, the problem in (9) can be a convex optimization problem.

## 5.2 Analytical Results

Since the objective function is convex, we are able to use the Lagrangian relaxation method for solving the problem in (9). In our work, we apply a novel *variable decoupling* technique for the replication sets  $\{A_m\}_{m=1}^M$  and  $\{B_m\}_{m=1}^M$ , which leads to a much simpler analysis without fundamentally losing order optimality, compared to tackling the original problem that may not provide a tractable closed-form solution. Notice that the total number of replicas of content object  $m \in \mathcal{M}$ ,  $A_m + B_m$ , can be simplified as  $\Theta(A_m)$  or  $\Theta(B_m)$  according to the relative size of  $A_m$  and  $B_m$ . For analytical convenience, given the optimal solution  $\{A_m^*\}_{m=1}^M$  and  $\{B_m^*\}_{m=1}^M$ , let us define two subsets  $\mathcal{M}_1$  and  $\mathcal{M}_2$  as the sets of content objects such that  $A_m^* + B_m^* = \Theta(A_m^*)$  and  $A_m^* + B_m^* = \Omega(f(n))$ , respectively, which will be specified in Theorem 2. We also define the subset  $\mathcal{M}_3$  as the set of content objects such that  $A_m^* + B_m^* = \Theta(B_m^*)$ . Note that for  $m \in \mathcal{M}_3$ ,  $A_m = O(B_m) = O(f(n))$ . Then, the optimization problem in (9) is divided into the following two optimization problems:

$$\min_{\{A_m\}_{m \in \mathcal{M}_1}} \sum_{m \in \mathcal{M}_1} \frac{p_m}{\sqrt{A_m}} \quad (10a)$$

$$\text{subject to } \sum_{m=1}^M A_m \leq nK_n, \quad (10b)$$

$$A_m \leq n \text{ for } m \in \mathcal{M}_1 \quad (10c)$$

and

$$\min_{\{B_m\}_{m \in \mathcal{M}_3}} \sum_{m \in \mathcal{M}_3} \frac{p_m}{\sqrt{B_m}} \quad (11a)$$

$$\text{subject to } \sum_{m=1}^M B_m \leq f(n)K_{FAP}, \quad (11b)$$

$$B_m \leq f(n) \text{ for } m \in \mathcal{M}_3. \quad (11c)$$

The Lagrangian function corresponding to (10) is given by

$$\begin{aligned} \mathcal{L}_1(\{A_m\}_{m \in \mathcal{M}_1}, \lambda, \{w_m\}_{m \in \mathcal{M}_1}) \\ = \sum_{m \in \mathcal{M}_1} \frac{p_m}{\sqrt{A_m}} + \lambda \left( \sum_{m=1}^M A_m - nK_n \right) + \sum_{m \in \mathcal{M}_1} w_m (A_m - n), \end{aligned} \quad (12)$$

where  $w_m, \lambda \in \mathbb{R}$ . The Karush–Kuhn–Tucker (KKT) conditions for (10) are then given by

$$\frac{\partial \mathcal{L}_1(\{A_m^*\}_{m \in \mathcal{M}_1}, \lambda^*, \{w_m^*\}_{m \in \mathcal{M}_1})}{\partial A_m^*} = 0 \quad (13)$$

$$\lambda^* \geq 0$$

$$w_m^* \geq 0$$

$$w_m^* (A_m^* - n) = 0 \quad (14)$$

$$\lambda^* \left( \sum_{m=1}^M A_m^* - nK_n \right) = 0 \quad (15)$$

for  $m \in \mathcal{M}_1$ . Similarly, the Lagrangian function corresponding to (11) is

$$\begin{aligned} \mathcal{L}_2(\{B_m\}_{m \in \mathcal{M}_3}, \mu, \{\nu_m\}_{m \in \mathcal{M}_3}) \\ = \sum_{m \in \mathcal{M}_3} \frac{p_m}{\sqrt{B_m}} + \mu \left( \sum_{m=1}^M B_m - f(n)K_{FAP} \right) + \sum_{m \in \mathcal{M}_3} \nu_m (B_m - f(n)), \end{aligned} \quad (16)$$



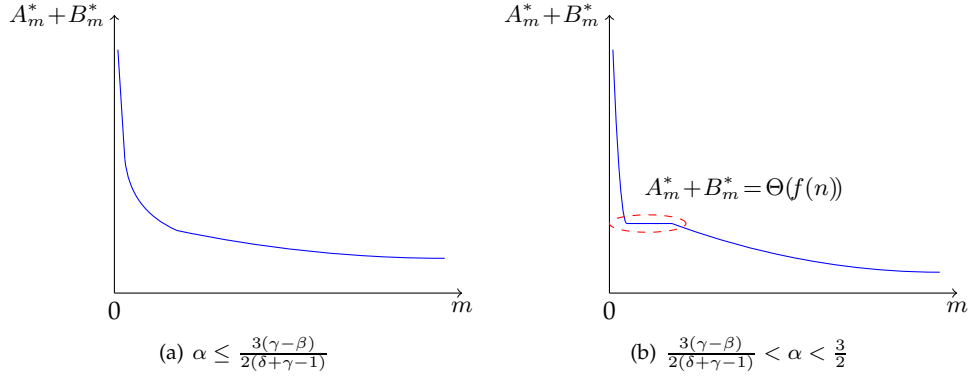


Fig. 3: The order-optimal cache allocation strategy with respect to the content object  $m$ .

where  $\nu_m, \mu \in \mathbb{R}$ . Then for  $\forall m \in \mathcal{M}_3$ , the KKT conditions for (11) state that

$$\begin{aligned}
 \frac{\partial \mathcal{L}_2(\{B_m^*\}_{m \in \mathcal{M}_3}, \mu^*, \{\nu_m^*\}_{m \in \mathcal{M}_3})}{\partial B_m^*} &= 0 \\
 \mu^* &\geq 0 \\
 \nu_m^* &\geq 0 \\
 \nu_m^*(B_m^* - f(n)) &= 0 \\
 \mu^* \left( \sum_{m=1}^M B_m^* - f(n)K_{FAP} \right) &= 0.
 \end{aligned} \tag{17}$$

We start from introducing the following lemma, which plays an important role in solving our content replication problem.

**Lemma 2.** *Suppose that  $\alpha < 3/2$  and the content delivery routing in Section 3 is used for the content-centric mobile hybrid IoT network. Then, the optimal solution to (10), denoted by  $A_m^*$ , is non-increasing with  $m \in \mathcal{M}_1$  and the optimal solution to (11), denoted by  $B_m^*$ , is non-increasing with  $m \in \mathcal{M}_3$ .*

*Proof:* Refer to Appendix A. □

From the above lemma, the following important theorem can be established, which shows the optimal total number of replicas of contents  $m \in \mathcal{M}$  at both mobile devices and static FAPs in terms of scaling laws.

**Theorem 2.** *Suppose that  $\alpha < 3/2$  and the content delivery routing in Section 3 is used for the content-centric mobile hybrid IoT network. If  $\alpha \leq \frac{3(\gamma-\beta)}{2(\delta+\gamma-1)}$ , then the order-optimal solution to (9) is given by*

$$A_m^* + B_m^* = \Theta \left( m^{-\frac{2\alpha}{3}} n^{\beta+\delta-\gamma(1-\frac{2\alpha}{3})} \right).$$

If  $\frac{3(\gamma-\beta)}{2(\delta+\gamma-1)} < \alpha < \frac{3}{2}$ , then it is given by

$$A_m^* + B_m^* = \begin{cases} \Theta \left( m^{-\frac{2\alpha}{3}} n^{\delta+(1-\delta)\frac{2\alpha}{3}} \right) & \text{for } m \in \mathcal{M}_1, \\ \Theta \left( n^\delta \right) & \text{for } m \in \mathcal{M}_2 \setminus \mathcal{M}_1, \\ \Theta \left( m^{-\frac{2\alpha}{3}} n^{\beta+\delta-\gamma(1-\frac{2\alpha}{3})} \right) & \text{for } m \in \mathcal{M} \setminus \mathcal{M}_2, \end{cases}$$

where  $\mathcal{M}_1 = \{1, \dots, m_1 - 1\}$  and  $\mathcal{M}_2 = \{1, \dots, m_2 - 1\}$ . Here,  $m_1 = \Theta(n^{1-\delta})$  and  $m_2 = \Theta(n^{\gamma-(\gamma-\beta)\frac{3}{2\alpha}})$ .

*Proof:* Refer to Appendix B. □

The order-optimal solution in Theorem 2 is illustrated in Fig. 3. For  $\alpha \leq \frac{3(\gamma-\beta)}{2(\delta+\gamma-1)}$ , the optimal number of replicas of content object  $m$ ,  $A_m^* + B_m^*$ , is shown to monotonically decrease with  $m$ . For  $\frac{3(\gamma-\beta)}{2(\delta+\gamma-1)} < \alpha < \frac{3}{2}$ , there exists a set of content objects such that  $A_m^* + B_m^*$  scales as  $\Theta(f(n))$ .

Now, we turn to describing our replication strategy by individually choosing the replication sets  $\{A_m^*\}_{m=1}^M$  and  $\{B_m^*\}_{m=1}^M$ . We introduce the following proposition, which exhibits that the resulting  $\{A_m^*\}_{m=1}^M$  and  $\{B_m^*\}_{m=1}^M$  still guarantee the order optimality as long as scaling laws are concerned.

**Proposition 1.** *Suppose that  $\alpha < \frac{3}{2}$  and the content delivery routing in Section 3 is used for the content-centric mobile hybrid IoT*

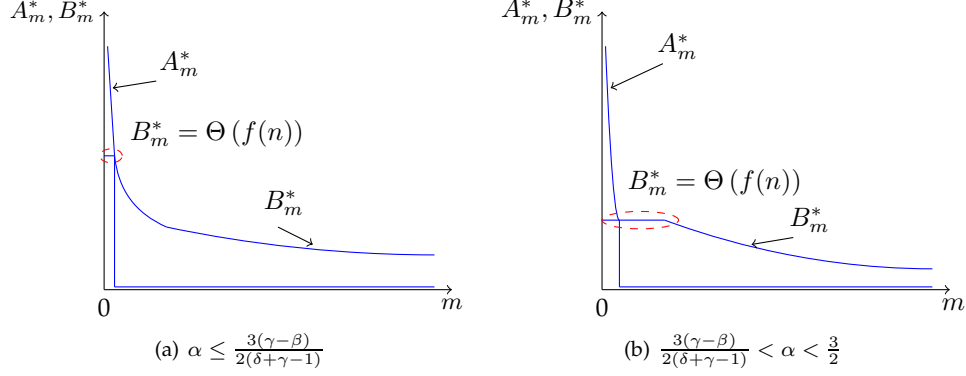


Fig. 4: The replication sets  $\{A_m^*\}_{m=1}^M$  and  $\{B_m^*\}_{m=1}^M$  with respect to the content object  $m$ .

network. Then, the order-optimal individual replication sets  $\{A_m^*\}_{m=1}^M$  and  $\{B_m^*\}_{m=1}^M$  are given by

$$A_m^* = \begin{cases} \Theta\left(m^{-\frac{2\alpha}{3}} n^{\min\{\beta+\delta-\gamma(1-\frac{2\alpha}{3}), \delta+(1-\delta)\frac{2\alpha}{3}\}}\right) & \text{for } m \in \mathcal{M}_1 \cap \mathcal{M}_2, \\ 0 & \text{for } m \in \mathcal{M} \setminus (\mathcal{M}_1 \cap \mathcal{M}_2) \end{cases} \quad (18)$$

and

$$B_m^* = \begin{cases} \Theta(n^\delta) & \text{for } m \in \mathcal{M}_2, \\ \Theta\left(m^{-\frac{2\alpha}{3}} n^{\beta+\delta-\gamma(1-\frac{2\alpha}{3})}\right) & \text{for } m \in \mathcal{M} \setminus \mathcal{M}_2, \end{cases}$$

respectively, where  $\mathcal{M}_1 = \{1, \dots, m_1 - 1\}$  and  $\mathcal{M}_2 = \{1, \dots, m_2 - 1\}$ . Here,  $m_1 = \Theta(n^{1-\delta})$  and  $m_2 = \Theta\left(n^{\gamma-(\gamma-\beta)\frac{3}{2\alpha}}\right)$ .

*Proof:* We prove the proposition by individually selecting  $\{A_m^*\}_{m=1}^M$  and  $\{B_m^*\}_{m=1}^M$  that satisfy the order-optimal solution  $\{A_m^* + B_m^*\}_{m=1}^M$  in Theorem 2 according to the following two cases depending on the value of  $\alpha$ .

Let us first focus on the case where  $\alpha \leq \frac{3(\gamma-\beta)}{2(\delta+\gamma-1)}$ . For  $m \in \mathcal{M}_2$  where  $A_m^* + B_m^* = \Omega(f(n)) (= \Omega(n^\delta))$ , we set  $A_m^* = \Theta\left(m^{-\frac{2\alpha}{3}} n^{\beta+\delta-\gamma(1-\frac{2\alpha}{3})}\right)$  and  $B_m^* = \Theta(n^\delta)$ . For  $\mathcal{M} \setminus \mathcal{M}_2$  where  $A_m^* + B_m^* = o(f(n))$ , we set  $A_m^* = 0$  and  $B_m^* = \Theta\left(m^{-\frac{2\alpha}{3}} n^{\beta+\delta-\gamma(1-\frac{2\alpha}{3})}\right)$ .

Next, we consider the case where  $\frac{3(\gamma-\beta)}{2(\delta+\gamma-1)} < \alpha < \frac{3}{2}$ . For  $m \in \mathcal{M}_1$  where  $A_m^* + B_m^* = \Theta(A_m^*)$ , we set  $A_m^* = \Theta\left(m^{-\frac{2\alpha}{3}} n^{\delta+(1-\delta)\frac{2\alpha}{3}}\right)$  and  $B_m^* = \Theta(n^\delta)$ . For  $m \in \mathcal{M}_2 \setminus \mathcal{M}_1$  where  $A_m^* + B_m^* = \Theta(f(n))$ , we set  $A_m^* = 0$  and  $B_m^* = \Theta(n^\delta)$ . As in the previous case, we also set  $A_m^* = 0$  and  $B_m^* = \Theta\left(m^{-\frac{2\alpha}{3}} n^{\beta+\delta-\gamma(1-\frac{2\alpha}{3})}\right)$  for  $m \in \mathcal{M} \setminus \mathcal{M}_2$ .

From the fact that  $m_1 = \Theta(n^{1-\delta})$  and  $m_2 = \Theta\left(n^{\gamma-(\gamma-\beta)\frac{3}{2\alpha}}\right)$ , it follows that  $\mathcal{M}_1 \cap \mathcal{M}_2 = \mathcal{M}_2$  if  $\alpha \leq \frac{3(\gamma-\beta)}{2(\delta+\gamma-1)}$ . Otherwise,  $\mathcal{M}_1 \cap \mathcal{M}_2 = \mathcal{M}_1$ . As a consequence, according to the above setting,  $A_m^*$  can be written in a single expression in (18). This completes the proof of the proposition.  $\square$

The order-optimal replication strategy in Proposition 1 is illustrated in Fig. 4. From this result, the following insightful observations are made.

**Remark 2.** From Fig. 4, it is observed that highly popular content objects, whose number of replicas is  $\omega(f(n))$ , are mainly served by device-to-device multihop routing while the rest of the content objects are served by deployed FAPs. More specifically, from Proposition 1, caching content objects  $m \in \mathcal{M}_1 \cap \mathcal{M}_2$  mostly at mobile devices is order-optimal in terms of throughput–delay trade-off. Thus, this replication strategy sheds light on how to cache in large-scale content-centric mobile hybrid IoT networks.

From Theorems 1 and 2 and Proposition 1, we characterize the order-optimal throughput–delay trade-off. To be specific, the objective function in (9a) is given by

$$\sum_{m=1}^M \frac{p_m}{\sqrt{A_m^* + B_m^*}} = \Theta\left(\frac{n^{\gamma(\frac{3}{2}-\alpha)-\frac{\beta+\delta}{2}}}{H_\alpha(M)}\right),$$

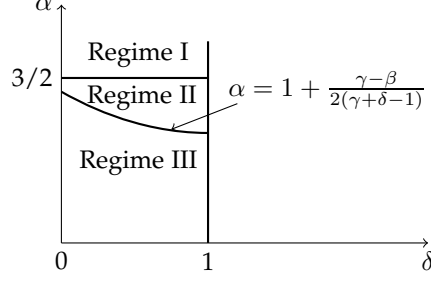


Fig. 5: The operating regimes on the throughput-delay trade-off with respect to  $\alpha$ ,  $\delta$ ,  $\beta$ , and  $\gamma$ .

where  $H_\alpha(M) = \sum_{i=1}^M i^{-\alpha}$ . For  $\frac{3(\gamma-\beta)}{2(\delta+\gamma-1)} < \alpha < \frac{3}{2}$ , we have

$$\begin{aligned}
& \sum_{m=1}^M \frac{p_m}{\sqrt{A_m^* + B_m^*}} \\
&= \sum_{m=1}^{m_1-1} \frac{p_m}{\sqrt{A_m^* + B_m^*}} + \sum_{m=m_1}^{m_2-1} \frac{p_m}{\sqrt{A_m^* + B_m^*}} + \sum_{m=m_2}^M \frac{p_m}{\sqrt{A_m^* + B_m^*}} \\
&= \Theta\left(\frac{n^{(1-\delta)(\frac{3}{2}-\alpha)-\frac{1}{2}}}{H_\alpha(M)}\right) + \Theta\left(\frac{n^{-\frac{\delta}{2}} \max\{H_\alpha(m_1), H_\alpha(m_2)\}}{H_\alpha(M)}\right) \\
&+ \Theta\left(\frac{n^{\gamma(\frac{3}{2}-\alpha)-\frac{\delta+\beta}{2}}}{H_\alpha(M)}\right). \tag{19}
\end{aligned}$$

Let the first, second, and third terms in the right-hand side of (19) be denoted by  $F_1$ ,  $F_2$ , and  $F_3$ , respectively. Then, it is seen that  $F_2 = \Theta(F_1)$  for  $1 < \alpha < \frac{3}{2}$  and  $F_2 = O(F_3)$  for  $\alpha \leq 1$ . In addition, for  $\alpha \leq \frac{3(\gamma-\beta)}{2(\delta+\gamma-1)}$ , the objective function  $\sum_{m=1}^M \frac{p_m}{\sqrt{A_m^* + B_m^*}}$  in (9a) is shown to scale as  $F_3$ . Thus, we need to compare the relative size of  $F_1$  and  $F_3$  according to the four scaling parameters  $\alpha$ ,  $\delta$ ,  $\beta$ , and  $\gamma$  to scrutinize the scaling behavior of (9a). In our work, we partition the entire parameter space, including the case where  $\alpha \geq \frac{3}{2}$ , into three operating regimes as follows (refer to Fig. 5).

- Regime I (High Zipf exponent regime):  $\{\alpha | \alpha \geq \frac{3}{2}\}$
- Regime II (Medium Zipf exponent regime):  $\left\{\alpha \left| 1 + \frac{\gamma-\beta}{2(\gamma+\delta-1)} \leq \alpha < \frac{3}{2} \right.\right\}$
- Regime III (Low Zipf exponent regime):  $\left\{\alpha \left| \alpha < 1 + \frac{\gamma-\beta}{2(\gamma+\delta-1)} \right.\right\}$

We are now ready to characterize the order-optimal throughput-delay trade-off in the following theorem.

**Theorem 3.** Suppose that the content delivery routing in Section 3 and the order-optimal replication strategy in Proposition 1 are used for the content-centric mobile hybrid IoT network. Then, according to the Zipf exponent  $\alpha$  and the scaling parameters  $\gamma$ ,  $\delta$ , and  $\beta$ , the order-optimal throughput-delay trade-off is given by

$$\lambda(n) = \Theta\left(\frac{D(n)}{n^b}\right), \text{ where } \lambda(n) = O\left(\frac{1}{\sqrt{n^{b+\epsilon}}}\right),$$

for an arbitrarily small constant  $\epsilon > 0$ . Here,

$$b = \begin{cases} 0 & \text{in Regime I,} \\ (1-\delta)(3-2\alpha) & \text{in Regime II,} \\ 1-\delta-\beta + \min\{3-2\alpha, 1\}\gamma & \text{in Regime III.} \end{cases}$$

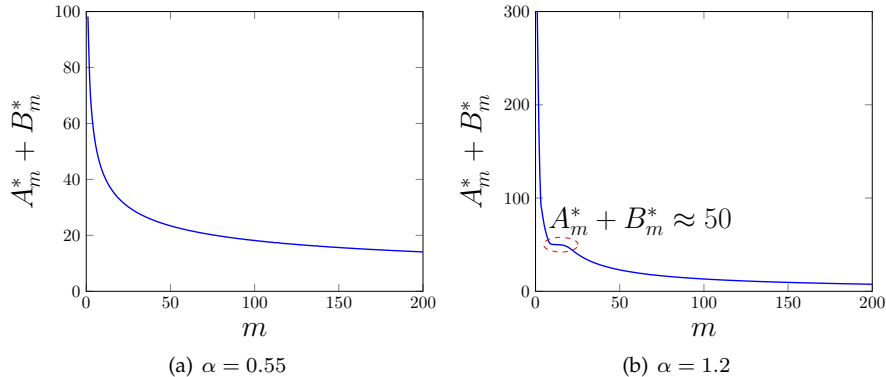
*Proof:* In Regime I,  $\lambda(n) = \Theta(D(n))$  is achieved. In Regime II, it is shown that (9a) scales as  $F_1 = \Theta\left(n^{(1-\delta)(\frac{3}{2}-\alpha)-\frac{1}{2}}\right)$ , thereby resulting in  $b = (1-\delta)(3-2\alpha)$  from (5). Now, let us turn to Regime III as follows: for  $1 < \alpha < 1 + \frac{\gamma-\beta}{2(\gamma+\delta-1)}$ , (9a) scales as  $F_3 = \Theta\left(n^{\gamma(\frac{3}{2}-\alpha)-\frac{\delta+\beta}{2}}\right)$ ; and for  $\alpha \leq 1$ , (9a) scales as  $F_3 = \Theta\left(n^{\frac{\gamma}{2}-\frac{\delta+\beta}{2}}\right)$ . Thus, we have  $b = 1 - \delta - \beta + \min\{3 - 2\alpha, 1\}$ . This completes the proof of the theorem.  $\square$

The impact and benefits of FAPs equipped with a finite-size cache are explicitly addressed according to each operating regime on the order-optimal throughput-delay trade-off.

**Remark 3.** In Regime I (i.e., the high Zipf exponent regime), the best performance  $\lambda(n) = \Theta(D(n))$  is achieved by using device-to-device multihop communication, and thus the use of FAPs does not further improve the performance. This is because highly popular contents objects are dominant in the regime. On the other hand, in Regimes II and III (i.e., the medium and low Zipf exponent

TABLE 1: The simulation environment

Symbol	Description	Value
$n$	The number of mobile devices	300
$M$	The size of the library	200
$f(n)$	The number of FAPs	50
$K_{FAP}$	The cache size of each FAP	50
$K_n$	The cache size of each device	2

Fig. 6: The optimal set  $\{A_m^* + B_m^*\}_{m=1}^{200}$  with respect to the content object  $m$ .

regimes), it turns out that the supplemental cache space  $f(n)K_{FAP}$  in the mobile hybrid IoT network significantly improves the network performance over the mobile IoT network with no FAP. Interestingly, in Regime II, the order-optimal trade-off is shown to be the same as in the content-centric static IoT network case assuming FAPs equipped with the infinite-size cache (or equivalently, the infinite-speed backhaul-aided cache) [26].

## 6 NUMERICAL EVALUATION

In this section, to validate the analytical results shown in Section 5.2, we perform intensive numerical evaluation by numerically solving the optimization problem in (9) according to finite values of the system parameters  $n$ ,  $M$ ,  $K_n$ ,  $K_{FAP}$ , and  $f(n)$  in Table 1, where the exponents  $\gamma$ ,  $\beta$ , and  $\delta$  are given by 0.93, 0.69, and 0.69, respectively. As in Section 5.2, we consider two cases  $\alpha \leq \frac{3(\gamma-\beta)}{2(\delta+\gamma-1)}$  and  $\frac{3(\gamma-\beta)}{2(\delta+\gamma-1)} < \alpha < \frac{3}{2}$ , where  $\frac{3(\gamma-\beta)}{2(\delta+\gamma-1)} = 0.59$ . To account for a distinct feature of the optimal solution to (9) in each case, the following two values of  $\alpha$  are used:  $\alpha = 0.55$  and  $\alpha = 1.2$ .

In Fig. 6, the set  $\{A_m^* + B_m^*\}_{m=1}^{200}$  is illustrated according to the content object  $m$ . It is found that the simulation results are consistent with our analytical trend in Theorem 2, which is depicted in Fig. 3. More specifically, for  $\alpha = 0.55$ , it is shown in Fig. 6(a) that  $A_m^* + B_m^*$  monotonically decreases as  $m$  increases. Besides, as illustrated in Fig. 6(b), there exists a set of content objects  $m$  such that  $A_m^* + B_m^*$  is approximately given by  $f(n) = 50$  for  $\alpha = 1.2$ .

In Fig. 7, the sets  $\{A_m^*\}_{m=1}^{200}$  and  $\{B_m^*\}_{m=1}^{200}$  are illustrated according to  $m$ . It is also found that the overall trends in the figure are similar to our analytical result in Proposition 1, which is depicted in Fig. 4. Our numerical results indicate that only a subset of highly popular content objects are mainly cached and delivered by mobile devices. It is also observed that  $B_m^*$  is close to  $f(n) = 50$  for small  $m$  and then decreases as  $m$  increases.

## 7 BASELINE STRATEGY IN MOBILE HYBRID IOT NETWORKS

Since our network model has never been studied before, we present our own baseline scheme that employs a rather naïve caching strategy. More specifically, we present a baseline cache allocation strategy, where the replication sets  $\{A_m\}_{m=1}^M$  and  $\{B_m\}_{m=1}^M$  are found by solving two separate optimization problems instead of our original problem in (9). We first present the problem formulation and then find the individual replication sets. Finally, performance comparison is conducted between two cache allocation strategies.

### 7.1 Problem Formulation

For the baseline approach, we consider two scenarios such that all content objects are stored *only at mobile devices* (i.e.,  $K_{FAP} = 0$ ) or *only at static FAPs* (i.e.,  $K_n = 0$ ). Then, the objective function (9a) boils down to  $\sum_{m=1}^M \frac{p_m}{\sqrt{A_m}}$  or  $\sum_{m=1}^M \frac{p_m}{\sqrt{B_m}}$ .

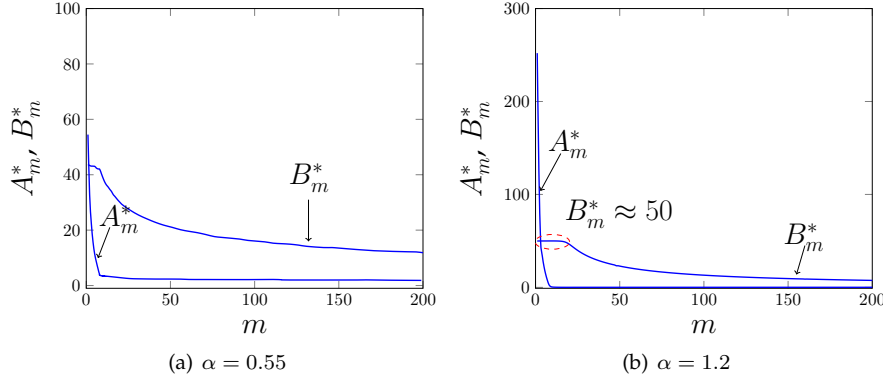


Fig. 7: The proposed individual replication sets  $\{A_m^*\}_{m=1}^{200}$  and  $\{B_m^*\}_{m=1}^{200}$  with respect to the content object  $m$ .

To be specific, two optimization problems can be formulated as follows:

$$\min_{\{A_m\}_{m=1}^M} \sum_{m=1}^M \frac{p_m}{\sqrt{A_m}} \quad (20a)$$

$$\text{subject to } \sum_{m=1}^M A_m \leq nK_n, \quad (20b)$$

$$1 \leq A_m \leq n \text{ for } m \in \mathcal{M} \quad (20c)$$

and

$$\min_{\{B_m\}_{m=1}^M} \sum_{m=1}^M \frac{p_m}{\sqrt{B_m}} \quad (21a)$$

$$\text{subject to } \sum_{m=1}^M B_m \leq f(n)K_{FAP}, \quad (21b)$$

$$1 \leq B_m \leq f(n) \text{ for } m \in \mathcal{M}. \quad (21c)$$

In the same manner used in Section 5, the discrete variables  $A_m$  and  $B_m$  are relaxed to real number in  $[1, \infty)$  to preserve the convexity of the objective functions (20a) and (21a).

## 7.2 Analytical Results

As in Section 5.2, we use the Lagrangian relaxation method for solving two optimization problems in (20) and (21). We establish the following theorem, which characterizes the optimal total number of replicas of content object  $m \in \mathcal{M}$ .

**Theorem 4.** *Suppose that  $\alpha < 3/2$  and the content delivery routing in Section 3 is used for the content-centric mobile hybrid IoT network. Then, the order-optimal solutions to (20) and (21) lead to*

$$A_m^* + B_m^* = \begin{cases} \Theta\left(m^{-\frac{2\alpha}{3}} n^{1-\gamma(1-\frac{2\alpha}{3})}\right) & \text{for } m \in \mathcal{M}_4, \\ \Theta\left(n^\delta\right) & \text{for } m \in \mathcal{M}_2 \setminus \mathcal{M}_4, \\ \Theta\left(m^{-\frac{2\alpha}{3}} n^{\beta+\delta-\gamma(1-\frac{2\alpha}{3})}\right) & \text{for } m \in \mathcal{M} \setminus \mathcal{M}_2, \end{cases}$$

where  $\mathcal{M}_2 = \{1, \dots, m_2 - 1\}$  and  $\mathcal{M}_4 = \{1, \dots, m_4 - 1\}$ . Here,  $m_2 = \Theta\left(n^{\gamma-(\gamma-\beta)\frac{3}{2\alpha}}\right)$  and  $m_4 = \Theta\left(n^{\gamma-(\gamma+\delta-1)\frac{3}{2\alpha}}\right)$ .

*Proof:* Since the first problem (20) corresponds to the optimization problem for the IoT network case with no FAP, the order-optimal replication set  $\{A_m^*\}_{m=1}^M$  is given by

$$A_m^* = \Theta\left(m^{-\frac{2\alpha}{3}} n^{1-\gamma(1-\frac{2\alpha}{3})}\right) \quad (22)$$

for  $\alpha < \frac{3}{2}$  [26].

Now, let us turn to solving the second problem (21), which corresponds to the scenario where content objects are stored only at FAPs. Using arguments similar to those in the proof of Theorem 2, it is not difficult to derive that  $B_m^* = \Theta(f(n)) = \Theta(n^\delta)$  for  $m \in \mathcal{M}_2 \triangleq \{1, \dots, m_2 - 1\}$  and

$$B_m^* = \Theta\left(m^{-\frac{2\alpha}{3}} n^{\beta+\delta-\gamma(1-\frac{2\alpha}{3})}\right) \quad (23)$$

for  $m \in \mathcal{M} \setminus \mathcal{M}_2$ , where  $m_2 = \Theta\left(n^{\gamma - (\gamma - \beta)\frac{3}{2\alpha}}\right)$ .

From (22) and (23), we next focus on deciding when each replication set  $A_m^*$  or  $B_m^*$  is dominant for all  $m \in \mathcal{M}$ . Under the given condition that  $\delta + \beta \geq 1$ , we have  $B_m^* = \Omega(A_m^*)$  for  $m \in \mathcal{M} \setminus \mathcal{M}_2$ . Let  $\mathcal{M}_4 \triangleq \{1, \dots, m_4 - 1\}$  denote the set of content objects such that  $A_m^* + B_m^* = \Theta(A_m^*)$  under our baseline strategy, where  $m_4 - 1$  is the largest index of the set  $\mathcal{M}_4$ . Then, using (22) and the fact that  $A_{m_4-1}^* = \Theta(B_{m_4-1}^*) = \Theta(n^\delta)$ , we have  $n^\delta = \Theta\left(m_4^{-\frac{2\alpha}{3}} n^{1 - \gamma(1 - \frac{2\alpha}{3})}\right)$ , which results in  $m_4 = \Theta\left(n^{\gamma - (\gamma + \delta - 1)\frac{3}{2\alpha}}\right)$ . This completes the proof of the theorem.  $\square$

Now, the above baseline strategy is compared with the order-optimal one in Section 5. The throughput–delay trade-off of the baseline strategy can be found by applying the result in Theorem 4 to the objective function (9a). As a consequence, we have

$$\begin{aligned}
& \sum_{m=1}^M \frac{p_m}{\sqrt{A_m^* + B_m^*}} \\
&= \sum_{m=1}^{m_4-1} \frac{p_m}{\sqrt{A_m^* + B_m^*}} + \sum_{m=m_4}^{m_2-1} \frac{p_m}{\sqrt{A_m^* + B_m^*}} + \sum_{m=m_2}^M \frac{p_m}{\sqrt{A_m^* + B_m^*}} \\
&= \Theta\left(\frac{n^{(\gamma - (\gamma + \delta - 1)\frac{1}{\alpha})(\frac{3}{2} - \alpha) - \frac{1}{2}}}{H_\alpha(M)}\right) + \Theta\left(\frac{n^{-\frac{\delta}{2}} \max\{H_\alpha(m_2), H_\alpha(m_4)\}}{H_\alpha(M)}\right) \\
&+ \Theta\left(\frac{n^{\gamma(\frac{3}{2} - \alpha) - \frac{\beta + \delta}{2}}}{H_\alpha(M)}\right). \tag{24}
\end{aligned}$$

Let the first, second, and third terms in the right-hand side of (24) be denoted by  $F_4$ ,  $F_5$ , and  $F_3$ , respectively. Then, it is seen that  $F_5 = \Theta(F_4)$  for  $1 < \alpha < \frac{3}{2}$  and  $F_5 = O(F_3)$  for  $\alpha \leq 1$ . Thus, by comparing the relative size of  $F_3$  and  $F_4$ , one can show that if  $\frac{3(\gamma + \delta - 1)}{3(\gamma + \delta - 1) - (\gamma - \beta)} \leq \alpha < \frac{3}{2}$ , then  $F_4 = \Omega(F_3)$ ; and  $F_4 = o(F_3)$  otherwise. Next, for comparison with the order-optimal strategy in Section 5, we take into account the following three cases according to the values of  $\alpha$ . For  $\alpha < \frac{3(\gamma + \delta - 1)}{3(\gamma + \delta - 1) - (\gamma - \beta)}$ , the objective function (9a) scales as  $F_3$ , which implies that both order-optimal and baseline strategies have the same throughput–delay trade-off. For  $\frac{3(\gamma + \delta - 1)}{3(\gamma + \delta - 1) - (\gamma - \beta)} \leq \alpha < 1 + \frac{\gamma - \beta}{2(\gamma + \delta - 1)}$  and  $1 + \frac{\gamma - \beta}{2(\gamma + \delta - 1)} \leq \alpha < \frac{3}{2}$ , (9a) scales as  $F_3$  and  $F_1$ , respectively, under the order-optimal strategy, while it scales as  $F_4$  under the baseline. Since  $F_4$  is greater than both  $F_3$  and  $F_1$  in these two cases, the order-optimal one provides a better throughput–delay trade-off for  $\frac{3(\gamma + \delta - 1)}{3(\gamma + \delta - 1) - (\gamma - \beta)} \leq \alpha < \frac{3}{2}$ . Therefore, the baseline cache allocation strategy is strictly suboptimal in terms of scaling laws.

**Remark 4.** The performance gain over the baseline approach basically comes from the fact that in our order-optimal cache allocation strategy, mobile devices can further cache highly popular content objects, whose number of replicas is larger than the number of static FAPs. This finally leads to the performance improvement in terms of throughput–delay trade-off when  $A_m^* + B_m^* = \omega(n^\delta)$ .

Note that for  $\alpha \geq \frac{3}{2}$  (corresponding to the case where the use of FAPs is not beneficial), the objective function (9a) scales as  $\frac{1}{\sqrt{n}}$  when the baseline strategy is used, which also exhibits the best throughput–delay trade-off in our network from the result of Theorem 1.

## 8 CONCLUDING REMARKS

This paper analyzed the order-optimal throughput–delay trade-off in content-centric mobile hybrid IoT networks, where each of mobile devices and static FAPs is equipped with a finite cache size. A content delivery routing was first proposed to characterize a fundamental throughput–delay trade-off. Then, the order-optimal cache allocation strategy, which jointly finds the number of replicas cached at mobile devices and static FAPs using a variable decoupling technique, was presented to achieve the order-optimal throughput–delay trade-off. Our analytical results were comprehensively validated by numerical evaluation.

Suggestions for further research includes characterizing the optimal throughput–delay trade-off in mobile IoT networks for the case where the size of each content object is considerably large and thus the per-hop time required for content delivery may be greater than the duration of each time slot.

## APPENDIX A

### PROOF OF LEMMA 2

Let us first prove that  $A_m^*$  is non-increasing with  $m \in \mathcal{M}_1$ . From (13), we have

$$-\frac{p_m}{2\sqrt{A_m^{*3}}} + \lambda^* + w_m^* = 0 \text{ for } m \in \mathcal{M}_1. \tag{A.1}$$

Let  $\mathcal{D}_1 \subset \mathcal{M}_1$  denote the set of content objects such that  $A_m^* = n$  and  $m_0$  denote the smallest index such that  $A_{m_0}^* < n$ . Now, consider any content object  $k \in \mathcal{D}_1$ . Then, using (A.1) and the fact that  $w_{m_0}^* = 0$ , we have  $\lambda^* = \frac{p_k}{2\sqrt{A_k^{*3}}} - w_k^* = \frac{p_{m_0}}{2\sqrt{A_{m_0}^{*3}}} > 0$ .

Since  $A_k^* = n$ ,  $A_{m_0}^* < n$ , and  $w_k^* \geq 0$ , we obtain  $p_k > p_{m_0}$ , thus resulting in  $k < m_0$  due to the feature of a Zipf popularity in (1). That is,  $\mathcal{D}_1 = \{1, 2, \dots, m_0 - 1\}$ . Furthermore, for  $m \in \mathcal{M}_1 \setminus \mathcal{D}_1$ , using (14) and (A.1), we have  $A_m^* = \frac{p_m^{\frac{2}{3}}}{(2\lambda^*)^{\frac{2}{3}}}$ , which decreases with  $m$ . Therefore,  $A_m^*$  is non-increasing with  $m \in \mathcal{M}_1$ .

Let us turn to proving that  $B_m^*$  is non-increasing with  $m \in \mathcal{M}_3$ . Let  $\mathcal{D}_2 \subset \mathcal{M}_3$  denote the set of content objects such that  $B_m^* = f(n)$  and  $\tilde{m}_0$  denote the smallest index such that  $B_{\tilde{m}_0}^* < f(n)$ . By applying the KKT conditions for (11) and the same approach as above, one can show that  $\mathcal{D}_2 = \{1, 2, \dots, \tilde{m}_0 - 1\}$  and  $B_m^* = \frac{p_m^{\frac{2}{3}}}{(2\mu^*)^{\frac{2}{3}}}$  for  $m \in \mathcal{M}_3 \setminus \mathcal{D}_2$ , which decreases with  $m$ . Therefore,  $B_m^*$  is non-increasing with  $m \in \mathcal{M}_3$ . This completes the proof of the lemma.

## APPENDIX B

### PROOF OF THEOREM 2

As shown in the proof of Lemma 2 (see Appendix A), applying the KKT conditions for (10) and (11), we have

$$A_m^* = \frac{p_m^{\frac{2}{3}}}{(2\lambda^*)^{\frac{2}{3}}} \text{ for } m \in \mathcal{M}_1 \setminus \mathcal{D}_1 \quad (\text{B.2})$$

and

$$B_m^* = \frac{p_m^{\frac{2}{3}}}{(2\mu^*)^{\frac{2}{3}}} \text{ for } m \in \mathcal{M}_3 \setminus \mathcal{D}_2, \quad (\text{B.3})$$

where  $\mathcal{D}_1 \subset \mathcal{M}_1$  and  $\mathcal{D}_2 \subset \mathcal{M}_3$  are the sets of content objects such that  $A_m^* = n$  and  $B_m^* = f(n)$ , respectively. From the proof of Lemma 2, recall that  $\mathcal{D}_1 = \{1, \dots, m_0 - 1\}$ , where  $m_0$  denotes the smallest index such that  $A_m^* < n$ . Using (15) and (17), one can show that  $\sum_{m=1}^M A_m^* = nK_n$  and  $\sum_{m=1}^M B_m^* = f(n)K_{FAP}$  due to the fact that  $\lambda^* > 0$  and  $\mu^* > 0$ , respectively, which will be used for computing the sum of  $A_m^* + B_m^*$  over some indices in  $\mathcal{M}$ .

The optimization problem (9) can be solved according to the following two cases depending on how the Lagrangian multiplier  $\lambda^*$  in (12) scales with the another one  $\mu^*$  in (16). In particular, we consider two cases where  $\lambda^* = \Theta(\mu^*)$  and  $\lambda^* \neq \Theta(\mu^*)$ , each of which corresponds to the cases where  $\alpha \leq \frac{3(\gamma-\beta)}{2(\delta+\gamma-1)}$  and  $\frac{3(\gamma-\beta)}{2(\delta+\gamma-1)} < \alpha < \frac{3}{2}$ .

**Case 1:** We first consider the case where  $\lambda^* = \Theta(\mu^*)$ . Using (B.2) and (B.3), one can show that  $A_m^* + B_m^*$  is computed as

$$A_m^* + B_m^* = \frac{p_m^{\frac{2}{3}}}{\xi^{\frac{2}{3}}}, \quad (\text{B.4})$$

where  $\xi = \Theta(\lambda^*) = \Theta(\mu^*)$  for  $\forall m \in \mathcal{M} \setminus \mathcal{D}_1$ . By adding up  $A_m^* + B_m^*$  in (B.4) over  $\forall m \in \mathcal{M} \setminus \mathcal{D}_1$  and using the fact that  $\xi^{\frac{2}{3}} = \frac{\sum_{l=m_0}^M p_l^{\frac{2}{3}}}{\sum_{l=m_0}^M (A_l^* + B_l^*)}$ , we obtain

$$\begin{aligned} A_m^* + B_m^* &= \frac{p_m^{\frac{2}{3}}}{\sum_{l=m_0}^M p_l^{\frac{2}{3}}} \sum_{l=m_0}^M (A_l^* + B_l^*) \\ &= \Theta \left( m^{-\frac{2\alpha}{3}} n^{\beta+\delta-\gamma(1-\frac{2\alpha}{3})} \right). \end{aligned} \quad (\text{B.5})$$

Here, the second equality holds since the cardinality of  $\mathcal{D}_1$  is  $O(1)$  due to the cache space  $K_n = \Theta(1)$ ;  $\sum_{l=m_0}^M (A_l^* + B_l^*) = \Theta(n^{\delta+\beta})$  from the assumption that  $\delta + \beta \geq 1$  as  $K_{FAP} = \Theta(n^\beta)$  and  $f(n) = \Theta(n^\delta)$ ; from (1) and (2),  $\sum_{l=m_0}^M p_l^{\frac{2}{3}} = \sum_{l=m_0}^M \frac{l^{-\frac{2\alpha}{3}}}{H_3^{\frac{2}{3}}(M)} = \Theta \left( \frac{M^{1-\frac{2\alpha}{3}}}{H_3^{\frac{2}{3}}(M)} \right)$  for  $\alpha < \frac{3}{2}$ ; and  $M = \Theta(n^\gamma)$ .

Now, we proceed with proving that the set  $\mathcal{D}_1$  does not exist by contradiction. Suppose that there exists  $\mathcal{D}_1$  (or equivalently  $m_0 > 1$ ). When the largest index in the set  $\mathcal{M}_2$  of content objects such that  $A_m^* + B_m^* = \Omega(f(n))$  is denoted as  $m_2 - 1$ , it follows that  $A_{m_2-1}^* + B_{m_2-1}^* = \Theta(f(n))$ . Using (B.5), we have  $f(n) = \Theta \left( (m_2 - 1)^{-\frac{2\alpha}{3}} n^{\beta+\delta-\gamma(1-\frac{2\alpha}{3})} \right)$ , which then yields

$$m_2 = \Theta \left( n^{\gamma-(\gamma-\beta)\frac{3}{2\alpha}} \right). \quad (\text{B.6})$$

Meanwhile, it is seen that  $\mathcal{M}_1 \setminus \mathcal{D}_1 = \{m_0, \dots, m_2 - 1\}$ . This is because the set  $\mathcal{M}_2$  belongs to  $\mathcal{M}_1$  from the fact that  $B_m^* \leq f(n)$ . By adding up  $A_m^* + B_m^*$  in (B.4) over all  $m \in \mathcal{M}_1 \setminus \mathcal{D}_1$ , we thus have

$$A_m^* + B_m^* = \Theta(A_m^*) = \frac{p_m^{\frac{2}{3}}}{\sum_{l=m_0}^{m_2-1} p_l^{\frac{2}{3}}} \sum_{l=m_0}^{m_2-1} \Theta(A_l^*),$$

which results in

$$A_{m_0}^* = \Theta \left( \frac{\sum_{l=m_0}^{m_2-1} A_l^*}{(m_2-1)^{1-\frac{2\alpha}{3}}} \right) \quad (\text{B.7})$$

when  $m = m_0$  due to the fact that from (1) and (2),  $\sum_{l=m_0}^{m_2-1} p_l^{\frac{2}{3}} = \sum_{l=m_0}^{m_2-1} \frac{l^{-\frac{2\alpha}{3}}}{H_{\frac{2}{3}}(M)} = \Theta \left( \frac{(m_2-1)^{1-\frac{2\alpha}{3}}}{H_{\frac{2}{3}}(M)} \right)$  for  $\alpha < \frac{3}{2}$ . Since  $(m_2-1)^{1-\frac{2\alpha}{3}} = \omega(1)$  from (B.6) and  $\sum_{l=m_0}^{m_2-1} A_l^* = O(n)$ , it follows that  $A_{m_0}^* = o(n)$  from (B.7), which contradicts another relation  $A_{m_0}^* = \Theta(n)$ . Hence, we conclude that  $\mathcal{D}_1$  does not exist (i.e.,  $m_0 = 1$ ).

In the following, we show that the condition  $\lambda^* = \Theta(\mu^*)$  is identical to  $\alpha \leq \frac{3(\gamma-\beta)}{2(\delta+\gamma-1)}$ . Using (B.5) and (B.6) as well as  $m_0 = 1$ , we have  $\sum_{m=1}^{m_2-1} (A_m^* + B_m^*) = \frac{\sum_{m=1}^{m_2-1} p_m^{\frac{2}{3}}}{\sum_{l=1}^M p_l^{\frac{2}{3}}} \sum_{l=1}^M (A_l^* + B_l^*) = \Theta \left( n^{\delta+\beta-(\gamma-\beta)(\frac{3}{2\alpha}-1)} \right)$ . Using the fact that  $\sum_{m=1}^{m_2-1} (A_m^* + B_m^*) = \sum_{m=1}^{m_2-1} \Theta(A_m^*) = O(n)$ , we obtain the following inequality:  $\delta + \beta - (\gamma - \beta) \left( \frac{3}{2\alpha} - 1 \right) \leq 1$ , which is equivalent to  $\alpha \leq \frac{3(\gamma-\beta)}{2(\delta+\gamma-1)}$ . Therefore, if  $\alpha \leq \frac{3(\gamma-\beta)}{2(\delta+\gamma-1)}$ , then

$$A_m^* + B_m^* = \Theta \left( m^{-\frac{2\alpha}{3}} n^{\beta+\delta-\gamma(1-\frac{2\alpha}{3})} \right) \text{ for } m \in \mathcal{M}.$$

**Case 2:** We turn our attention to the case where  $\lambda^* \neq \Theta(\mu^*)$ . From (B.2) and (B.3), it is found that the two sets  $\mathcal{M}_1 \setminus \mathcal{D}_1$  and  $\mathcal{M}_3 \setminus \mathcal{D}_2$  do not share any common content object. Thus, it follows that  $\mathcal{M}_1 \subset \mathcal{M}_2$ . Based on this observation, we have

$$A_m^* + B_m^* = \Theta(B_m^*) = \Theta \left( n^\delta \right) \quad (\text{B.8})$$

for  $m \in \mathcal{M}_2 \setminus \mathcal{M}_1$ . For the sake of analytical convenience, by defining  $m_1 - 1$  and  $m_2 - 1$  as the largest indices in the sets  $\mathcal{M}_1$  and  $\mathcal{M}_2$ , respectively, we compute  $A_m^* + B_m^*$  for  $m \in \mathcal{M}_1$  and  $m \in \mathcal{M} \setminus \mathcal{M}_2$ .

First, we focus on finding both  $A_m^* + B_m^*$  and  $m_2$  for  $m \in \mathcal{M} \setminus \mathcal{M}_2$ , where  $\mathcal{M} \setminus \mathcal{M}_2 = \{m_2, \dots, M\}$ . By adding up  $B_m^*$  in (B.3) over all  $m \in \mathcal{M} \setminus \mathcal{M}_2$ , we have

$$B_m^* = \frac{p_m^{\frac{2}{3}}}{\sum_{l=m_2}^M p_l^{\frac{2}{3}}} \sum_{l=m_2}^M B_l^* \quad (\text{B.9a})$$

$$= O \left( m^{-\frac{2\alpha}{3}} n^{\delta+\beta-\gamma(1-\frac{2\alpha}{3})} \right), \quad (\text{B.9b})$$

where the second equality holds since  $\sum_{l=m_2}^M B_l^* = O(n^{\delta+\beta})$ ; from (1) and (2),  $\sum_{l=m_2}^M p_l^{\frac{2}{3}} = \sum_{l=m_2}^M \frac{l^{-\frac{2\alpha}{3}}}{H_{\frac{2}{3}}(M)} = \Theta \left( \frac{M^{1-\frac{2\alpha}{3}}}{H_{\frac{2}{3}}(M)} \right)$  for  $\alpha < \frac{3}{2}$ ; and  $M = \Theta(n^\gamma)$ . From (B.9b) and  $B_{m_2}^* = \Theta(f(n))$ , we have  $f(n) = O \left( m_2^{-\frac{2\alpha}{3}} n^{\delta+\beta-\gamma(1-\frac{2\alpha}{3})} \right)$ , which leads to  $m_2 = O \left( n^{\gamma - (\gamma-\beta)\frac{3}{2\alpha}} \right)$ . Since  $(\gamma - \beta) \left( 1 - \frac{3}{2\alpha} \right) < 0$  under our network model, it follows that  $\gamma - (\gamma - \beta) \frac{3}{2\alpha} < \beta$ , thus resulting in  $m_2 = o(K_{FAP})$ . Because  $\sum_{l=m_2}^M B_l^* = f(n)K_{FAP} - O(m_2 f(n)) = \Theta(n^{\delta+\beta})$ , (B.9a) can be rewritten as

$$A_m^* + B_m^* = \Theta(B_m^*) = \Theta \left( m^{-\frac{2\alpha}{3}} n^{\delta+\beta-\gamma(1-\frac{2\alpha}{3})} \right) \quad (\text{B.10})$$

for  $m \in \mathcal{M} \setminus \mathcal{M}_2$ . Moreover, using the fact that  $A_{m_2}^* + B_{m_2}^* = \Theta \left( m_2^{-\frac{2\alpha}{3}} n^{\delta+\beta-\gamma(1-\frac{2\alpha}{3})} \right)$  from (B.10) and  $A_{m_2}^* + B_{m_2}^* = \Theta(f(n))$ , we obtain

$$m_2 = \Theta \left( n^{\gamma - (\gamma-\beta)\frac{3}{2\alpha}} \right). \quad (\text{B.11})$$

Next, we turn to finding both  $A_m^* + B_m^*$  and  $m_1$  for  $m \in \mathcal{M}_1$ . By adding up  $A_m^*$  in (B.2) over  $\forall m \in \mathcal{M}_1 \setminus \mathcal{D}_1 (= \{m_0, \dots, m_1 - 1\})$ , we have

$$A_m^* = \frac{p_m^{\frac{2}{3}}}{\sum_{l=m_0}^{m_1-1} p_l^{\frac{2}{3}}} \sum_{l=m_0}^{m_1-1} A_l^*. \quad (\text{B.12})$$

Similarly as in Case 1, we are capable of proving that  $\mathcal{D}_1$  does not exist (i.e.,  $m_0 = 1$ ). Because  $f(n) = \Theta \left( \frac{m_1^{-\frac{2\alpha}{3}} \sum_{l=1}^{m_1-1} A_l^*}{(m_1-1)^{1-\frac{2\alpha}{3}}} \right)$

due to  $\sum_{l=1}^{m_1-1} p_l^{\frac{2}{3}} = \Theta \left( \frac{(m_1-1)^{1-\frac{2\alpha}{3}}}{H_{\frac{2}{3}}(M)} \right)$  and  $A_{m_1-1}^* = \Theta(f(n))$ , it is not difficult to show that

$$m_1 = \Theta \left( \frac{\sum_{l=1}^{m_1-1} A_l^*}{f(n)} \right). \quad (\text{B.13})$$

Now, we need to specify the term  $\sum_{l=1}^{m_1-1} A_l^*$  to find  $m_1$ . For  $\alpha < \frac{3}{2}$ , by setting  $m_0 = 1$ , the objective function (9a) can be



expressed as

$$\begin{aligned}
& \sum_{m=1}^M \frac{p_m}{\sqrt{A_m^* + B_m^*}} \\
&= \sum_{m=1}^{m_1-1} \frac{p_m}{\sqrt{A_m^* + B_m^*}} + \sum_{m=m_1}^{m_2-1} \frac{p_m}{\sqrt{A_m^* + B_m^*}} + \sum_{m=m_2}^M \frac{p_m}{\sqrt{A_m^* + B_m^*}} \\
&= \Theta \left( \frac{\left( \sum_{m=1}^{m_1-1} p_m \right)^{\frac{2}{3}}}{\sqrt{\sum_{m=1}^{m_1-1} A_m^*}} \right) + \Theta \left( \frac{\sum_{m=m_1}^{m_2-1} p_m}{\sqrt{f(n)}} \right) + \Theta \left( \frac{\left( \sum_{m=m_2}^M p_m \right)^{\frac{2}{3}}}{\sqrt{\sum_{m=m_2}^M B_m^*}} \right) \\
&= \Theta \left( \frac{m_1^{1-\alpha}}{H_\alpha(M) \sqrt{f(n)}} \right) + \Theta \left( \frac{\max\{H_\alpha(m_1), H_\alpha(m_2-1)\}}{H_\alpha(M) \sqrt{f(n)}} \right) \\
&+ \Theta \left( \frac{M^{3/2-\alpha}}{H_\alpha(M) \sqrt{f(n) K_{FAP}}} \right), \tag{B.14}
\end{aligned}$$

where the second equality follows from (B.8) for  $m \in \mathcal{M}_2 \setminus \mathcal{M}_1$ , (B.9a) for  $m \in \mathcal{M} \setminus \mathcal{M}_2$ , and (B.12) for  $m \in \mathcal{M}_1$ ; the third equality holds since  $m_2 = o(M)$  from (B.11) as well as  $\sum_{l=1}^{m_1-1} p_l^{\frac{2}{3}} = \Theta \left( \frac{(m_1-1)^{1-\frac{2\alpha}{3}}}{H_\alpha^{\frac{2}{3}}(M)} \right)$  and  $\sum_{l=m_2}^M p_l^{\frac{2}{3}} = \Theta \left( \frac{M^{1-\frac{2\alpha}{3}}}{H_\alpha^{\frac{2}{3}}(M)} \right)$  from (1) and (2). One can show that the second term in (B.14) scales slower than the other two terms because for  $\alpha \leq 1$ , (9a) is given by the third term in (B.14) and for  $1 < \alpha < \frac{3}{2}$ , (9a) is dominated by either the first or the third term in (B.14). Since for  $1 < \alpha < \frac{3}{2}$ , the first term (including  $m_1$ ) can be minimized when  $m_1$  is maximized, it follows that  $\sum_{l=1}^{m_1-1} A_l^* = \Theta(n)$  from (3) (the total caching constraint) and (B.13). Accordingly, we have

$$m_1 = \Theta(n^{1-\delta}).$$

Moreover by setting  $m_0 = 1$ ,  $\sum_{l=1}^{m_1-1} p_l^{\frac{2}{3}} = \Theta \left( \frac{m_1^{1-\frac{2\alpha}{3}}}{H_\alpha^{\frac{2}{3}}(M)} \right)$ , and  $\sum_{l=1}^{m_1-1} A_l^* = \Theta(n)$ , (B.12) can be rewritten as

$$A_m^* + B_m^* = \Theta(A_m^*) = \Theta \left( m^{-\frac{2\alpha}{3}} n^{\delta+(1-\delta)\frac{2\alpha}{3}} \right) \text{ for } m \in \mathcal{M}_1.$$

As the last case, for  $m \in \mathcal{M}_2 \setminus \mathcal{M}_1$ ,  $A_m^* + B_m^*$  is obviously given by  $\Theta(n^\delta)$  from the definitions of  $\mathcal{M}_1$  and  $\mathcal{M}_2$ .

Finally, from the last paragraph of Case 1, it is obvious that  $\lambda^* \neq \Theta(\mu^*)$  when  $\frac{3(\gamma-\beta)}{2(\delta+\gamma-1)} < \alpha < \frac{3}{2}$ . This completes the proof of the theorem.

## REFERENCES

- [1] T.-A. Do, S.-W. Jeon, and W.-Y. Shin, "Caching in mobile HetNets: A throughput-delay trade-off perspective," in *Proc. IEEE Int. Symp. Inf. Theory (ISIT)*, Barcelona, Spain, Jul. 2016, pp. 1247-1251.
- [2] M. Ji, G. Caire, and A. F. Molisch, "Wireless device-to-device caching networks: Basic principles and system performance," *IEEE J. Sel. Areas Commun.*, vol. 34, no. 1, pp. 176-189, Jan. 2016.
- [3] M. Agiwal, A. Roy, and N. Saxena, "Next generation 5G wireless networks: A comprehensive survey," *IEEE Commun. Surveys Tuts.*, vol. 18, no. 3, pp. 1617-1655, Third Quart., 2016.
- [4] X. Li, X. Wang, K. Li, and V. C. M. Leung, "CaaS: Caching as a service for 5G networks," *IEEE Access*, vol. 5, pp. 5982-5993, Mar. 2017.
- [5] S. Wang, X. Zhang, Y. Zhang, L. Wang, J. Yang, and W. Wang, "A survey on mobile edge networks: Convergence of computing, caching and communications," *IEEE Access*, vol. 5, pp. 6757-6779, Mar. 2017.
- [6] P. Gupta and P. R. Kumar, "The capacity of wireless networks," *IEEE Trans. Inf. Theory*, vol. 46, no. 2, pp. 388-404, Mar. 2000.
- [7] M. Franceschetti, O. Dousse, D. N. C. Tse, and P. Thiran, "Closing the gap in the capacity of wireless networks via percolation theory," *IEEE Trans. Inf. Theory*, vol. 53, no. 3, pp. 1009-1018, Mar. 2007.
- [8] P. Gupta and P. R. Kumar, "Towards an information theory of large networks: An achievable rate region," *IEEE Trans. Inf. Theory*, vol. 49, no. 8, pp. 1877-1894, Aug. 2003.
- [9] F. Xue, L.-L. Xie, and P. R. Kumar, "The transport capacity of wireless networks over fading channels," *IEEE Trans. Inf. Theory*, vol. 51, no. 3, pp. 834-847, Mar. 2005.
- [10] W.-Y. Shin, S.-Y. Chung, and Y. H. Lee, "Parallel opportunistic routing in wireless networks," *IEEE Trans. Inf. Theory*, vol. 59, no. 10, pp. 6290-6300, Oct. 2013.
- [11] A. Özgür, O. Lévêque, and D. N. C. Tse, "Hierarchical cooperation achieves optimal capacity scaling in ad hoc networks," *IEEE Trans. Inf. Theory*, vol. 53, no. 10, pp. 3549-3572, Oct. 2007.
- [12] M. Grossglauser and D. N. C. Tse, "Mobility increases the capacity of ad hoc wireless networks," *IEEE/ACM Trans. Netw.*, vol. 10, no. 4, pp. 477-486, Aug. 2002.
- [13] A. El Gamal, J. Mammen, B. Prabhakar, and D. Shah, "Optimal throughput-delay scaling in wireless networks-Part I: The fluid model," *IEEE Trans. Inf. Theory*, vol. 52, no. 6, pp. 2568-2592, Jun. 2006.
- [14] G. Zhang, Y. Xu, X. Wang, and M. Guizani, "Capacity of hybrid wireless networks with directional antennas and delay constraint," *IEEE Trans. Commun.*, vol. 58, no. 7, pp. 2097-2106, July 2010.
- [15] P. Li, C. Zhang, and Y. Fang, "The capacity of wireless ad hoc networks using directional antennas," *IEEE Trans. Mobile Comput.*, vol. 10, no. 10, pp. 1374-1387, Oct. 2011.
- [16] J. Yoon, W.-Y. Shin, and S.-W. Jeon, "Elastic routing in ad hoc networks with directional antennas," *IEEE Trans. Mobile Comput.*, vol. 16, no. 12, pp. 3334-3346, Dec. 2017.

- [17] B. Liu, Z. Liu, and D. Towsley, "On the capacity of hybrid wireless networks," in *Proc. IEEE INFOCOM*, San Francisco, CA, Mar./Apr. 2003, pp. 1543–1552.
- [18] W.-Y. Shin, S.-W. Jeon, N. Devroye, M. H. Vu, S.-Y. Chung, Y. H. Lee, and V. Tarokh, "Improved capacity scaling in wireless networks with infrastructure," *IEEE Trans. Inf. Theory*, vol. 57, no. 8, pp. 5088–5102, Aug. 2011.
- [19] S. Gitseniz, G. S. Paschos, and L. Tassiulas, "Asymptotic laws for joint content replication and delivery in wireless networks," *IEEE Trans. Inf. Theory*, vol. 59, no. 5, pp. 2760–2776, May. 2013.
- [20] M. Ji, G. Caire, and A. F. Molisch, "The throughput-outage tradeoff of wireless one-hop caching networks," *IEEE Trans. Inf. Theory*, vol. 61, no. 12, pp. 6833–6859, Dec. 2015.
- [21] S.-W. Jeon, S.-N. Hong, M. Ji, G. Caire, and A. F. Molisch, "Wireless multihop device-to-device caching networks," *IEEE Trans. Inf. Theory*, vol. 63, no. 3, pp. 1662–1676, Mar. 2017.
- [22] G. Alfano, M. Garetto, and E. Leonardi, "Content-centric wireless networks with limited buffers: When mobility hurts," *IEEE/ACM Trans. Netw.*, vol. 24, no. 1, pp. 299–311, Feb. 2016.
- [23] A. Malik, S. H. Lim, and W.-Y. Shin, "On the effects of subpacketization in content-centric mobile networks," *IEEE J. Sel. Areas Commun.*, to appear.
- [24] X. Liu, K. Zheng, J. Zhao, X.-Y. Liu, X. Wang, and X. Di, "Information-centric networks with correlated mobility," *IEEE Trans. Veh. Technol.*, vol. 66, no. 5, pp. 4256–4270, May 2017.
- [25] G. Zhang, J. Liu, J. Ren, L. Wang, and J. Zhang, "Capacity of content-centric hybrid wireless networks," *IEEE Access*, vol. 5, pp. 1449–1459, Feb. 2017.
- [26] M. Mahdian and E. Yeh, "Throughput and delay scaling of content-centric ad hoc and heterogeneous wireless networks," *IEEE/ACM Trans. Netw.*, vol. 25, no. 5, pp. 3030–3043, Aug. 2017.
- [27] M. A. Maddah-Ali and U. Niesen, "Fundamental limits of caching," *IEEE Trans. Inf. Theory*, vol. 60, no. 5, pp. 2856–2867, May. 2014.
- [28] M. A. Maddah-Ali and U. Niesen, "Decentralized coded caching attains order-optimal memory-rate tradeoff," *IEEE/ACM Trans. Netw.*, vol. 23, no. 4, pp. 1029–1040, Aug. 2014.
- [29] M. A. Maddah-Ali and U. Niesen, "Coding for caching: Fundamental limits and practical challenges," *IEEE Commun. Mag.*, vol. 54, no. 8, pp. 23–29, Aug. 2016.
- [30] D. E. Knuth, "Big Omicron and big Omega and big Theta," *ACM SIGACT News*, vol. 8, no. 2, pp. 18–24, Apr.-Jun. 1976.
- [31] L. Zhou, R. Q. Hu, Y. Qian, and H.-H. Chen, "Energy-spectrum efficiency tradeoff for video streaming over mobile ad hoc networks," *IEEE J. Sel. Areas Commun.*, vol. 31, no. 5, pp. 981–991, May. 2013.
- [32] C. Fricker, P. Robert, J. Roberts, and N. Sbihi, "Impact of traffic mix on caching performance in a content-centric network," in *Proc. IEEE INFOCOM Workshop on Emerging Choices in Named-Oriented Netw. (NoMEN)*, Orlando, FL, Mar. 2012, pp. 310–315.
- [33] S. Lim, W.-C. Lee, G. Cao, and C. R. Das, "A novel caching scheme for Internet based mobile ad hoc networks," in *Proc. IEEE Computer Commun. and Netw. (ICCCN)*, Dallas, TX, USA, Oct. 2003, pp. 38–43.
- [34] M. X. Goemans, L. Li, V. S. Mirrokni, and M. Tholtan, "Market sharing games applied to content distribution in ad hoc networks," *IEEE J. Sel. Areas Commun.*, vol. 24, no. 5, pp. 1020–1033, May. 2006.